# Manipulation of a Rigid Body with a Flexible Sheet and its Application to a Rehabilitation Bed

by

Binayak Roy

B. Tech., Manufacturing Science and Engineering
IIT KHARAGPUR, 2001

SUBMITTED TO THE DEPARTMENT OF MECHANICAL ENGINEERING
IN PARTIAL FULFILLMENT OF THE REQUIREMENT FOR THE DEGREE OF

MASTER OF SCIENCE IN MECHANICAL ENGINEERING
AT THE
MASSACHUSETTS INSTITUTE OF TECHNOLOGY

September 2003





Signature of Author .....
Department of Mechanical Engineering
August 8, 2003

Certified by .....
Haruhiko H. Asada
Professor of Mechanical Engineering
Thesis Supervisor

Accepted by .....
Ain A. Sonin
Chairman, Department Committee on Graduate Students

# Manipulation of a Rigid Body with a Flexible Sheet and its Application to a Rehabilitation Bed

by

Binayak Roy

Submitted to the Department of Mechanical Engineering
on August 8, 2003 in partial fulfillment of the
requirements for the Degree of Master of Science in
Mechanical Engineering

## ABSTRACT

A new method for manipulation of a rigid body using a flexible sheet is presented. A key feature of the proposed system is that the body is not securely connected to the sheet and the contact region between the body and the sheet changes dynamically during manipulation. The use of a soft flexible sheet and the untethered nature of manipulation, makes the system particularly well suited to handling the human body. We present an application to a rehabilitation bed for repositioning a bedridden patient to alleviate secondary ailments such as bedsores. In order to prevent injury to the patient's fragile skin, it must be ensured that the patient does not slip on the sheet during repositioning. We model the system and present a no-slip condition based on system parameters. The model is used to develop a control strategy for coordinating the motions of multiple actuators of the prototype bed. The prototype bed can successfully reposition test subjects using the control strategy developed.

Thesis Supervisor: Haruhiko H. Asada

Title: Professor of Mechanical Engineering

# ACKNOWLEDGMENTS

I am grateful to Prof. Asada for his guidance at all stages of work during the preparation of this thesis. I am also thankful to my lab mates, especially Arin, Kyu Jin and Eric, for all the help and support that they have extended to me. Thanks also to Abhijit Guria for the many helpful discussions on the phone. Last but not the least, my sincere thanks to the support team back home.

## TABLE OF CONTENTS

# Chapter 1
# INTRODUCTION

## 1.1 Overview

Patients confined to the bed for a long period of time need to be periodically turned and repositioned to avoid painful bedsores and pneumonia [5]. The extended stay in hospitals due to these secondary ailments amounts to monetary damage of up to $55Bn per year [10]. Bedsores are formed due to lack of blood circulation caused by local pressure concentrations on a patient's body. Viral pneumonia is the result of lower respiratory infection and has been the cause of more than 90% of deaths for individuals over 65. Stagnant mucus in the lower airways is a medium for bacterial growth, should pathogens reach the lower airways. An effective remedial measure is to reposition the patient at regular intervals to ensure frequent pressure redistribution. Routine turning and repositioning also assists in mobilization of secretions. Additionally, patients having breathing difficulties may find relief by being turned slightly on their side [7].

The current practice in hospitals involves nursing personnel, who move the patients manually. Fig. 1.1 shows the typical steps involved in repositioning a bedridden patient. The patient is first pulled to one side of the bed using a draw sheet to ensure that she is centrally located on the bed after repositioning. In the next step, the patient is semi-turned and finally propped with pillows to support the final posture. This is a fairly labor

intensive task, with at least two caregivers involved for each patient. There is an acute shortage of nursing personnel and the current workforce frequently suffers back injuries, which cost up to $24Bn every year [13]. The repositioning operation is also time consuming and due to the aforementioned shortage, the patients do not get adequate attention leading to aggravation of the secondary ailments.

There are a few commercially available beds that fulfill some requirements of patients and nursing personnel. *Hill-Rom* [8] and *Kinetic Concepts Inc. (KCI)* [9] are some of the companies that make hospital beds. Some Japanese researchers have developed a rolling air cushion bed, which turns the patient to a 15-degree inclined lateral position with an inflating ripple mattress. The beds range from manually operated to electrical ones, some even equipped with fluidized therapy units that provide local pressure relief. However, these beds cannot really mimic the repositioning task shown in Fig. 1.1.

Basmajian et al [19] developed an approach for maneuvering a bedridden patient, which retains the use of the bed sheet but without the associated manual labor. They proposed and prototyped a novel design which can be used to periodically reposition a bedridden patient under the supervision of a single caregiver. Fig. 1.2 shows a schematic of the patient lying on a hammock-like bed cradled by the bed sheet. The rollers to which the ends of the bed sheet are attached were actuated with motors and thus the bed sheet could be rolled up or released so as to position the patient as desired. The details of the operation are elaborated in a later section. The maneuvering scheme precludes dragging the patient on the bed and thus reduces chances of injury to the patient's fragile skin through shear forces.

However, the problem was not adequately modeled and it would be difficult to maneuver the patient automatically. The maneuvering operation involved co-ordination of the actuators and this would depend completely on the judgment and skill of the caregiver, thus involving a considerable amount of time. The rehabilitation bed permitted semi-automated operation when it was preprogrammed. The program would have to be customized for patients of various sizes. The main difficulty was that the system would have to be reprogrammed to perform a repositioning operation depending on the initial location of the patient. This would once again considerably increase the set-up time of the device. Also, the position of the patient is not continuously monitored and thus the safety of the patient cannot be guaranteed should they willfully change their position during the repositioning operation or otherwise.

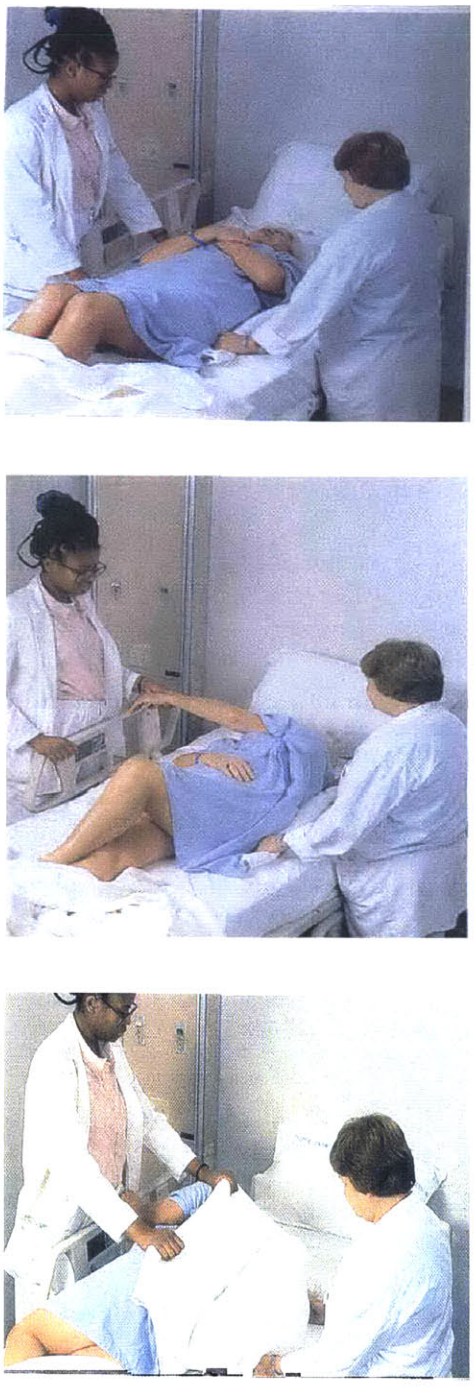

**Fig. 1.1. Steps involved in manual repositioning of a bedridden patient**

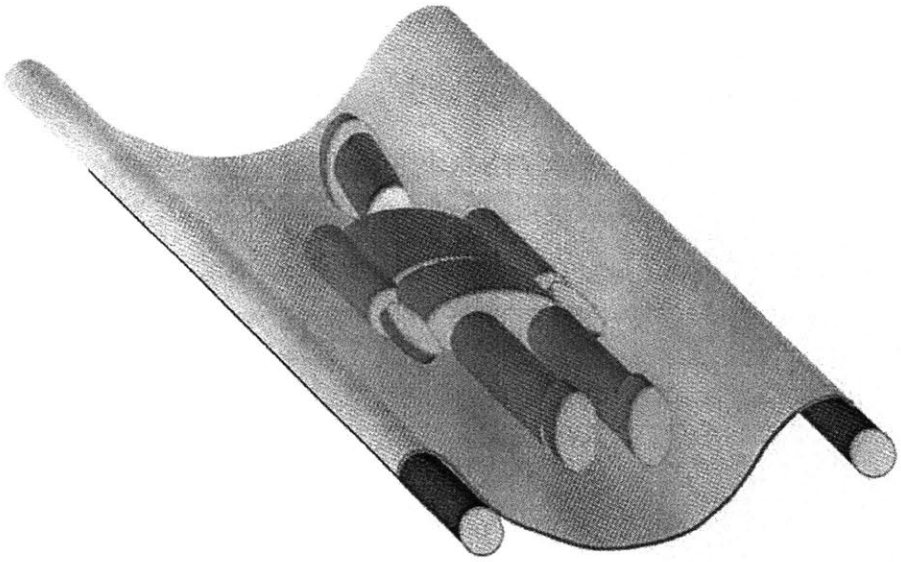

**Fig. 1.2. Schematic of patient on bed sheet**

In order to fulfill the above-mentioned requirements, we have to study and model the manipulation of objects using flexible sheets. Unlike traditional manipulation tasks performed by rigid robotic manipulators, handling a patient's body with a bed sheet is intricate due to the flexibility (negligible bending stiffness) of the bed sheet as well as the need for special care in handling human beings. The problem of handling objects using flexible cables is well studied in the context of container cranes, which are used primarily for cargo handling [1] [2] [3] [4]. Donald *et al.* have studied another aspect of this problem, which involves distributed manipulation of objects by wrapping ropes around them, focusing on wrapping algorithms and robot cooperation [20].

Our problem is fundamentally different from the above-mentioned cases. We must exercise special care while maneuvering the human body. Firstly, it cannot be hooked or securely tethered during manipulation, as is the case with cargo handling using container cranes. At the same time, we must ensure that the body does not slip relative to the sheet

as this can cause severe damage to the already fragile skin of bedridden patients. Secondly, to ensure the safety and comfort of the patient, the repositioning operation must be performed sufficiently slowly. Thus, speed and hence anti-swing control is a critical issue for container cranes, but is of little importance to us.

## 1.2 Summary of Design Concept

The design concept and some of the motivations behind the design of the prototype bed (designed and built by Arin Basmajian) are summarized in this section so that the modeling and analysis in the following chapters can be readily understood. The details can be found in [19].

As mentioned in the previous section, the bed was designed to maneuver bedridden patient using the bed sheet, as is done by nursing personnel. Some of the important factors that were taken into consideration were quick setup times, safety and acceptability. The setup time of the device should be small because caregivers may not wish to spend too much time setting up a machine for doing a task that requires a fraction of the time required to set it up. The safety of the patient is a top priority. Therefore, the device should conform to safety standards. It should also be deemed acceptable in hospital use by patients and nursing personnel.

As shown in Fig. 1.3, the design consists of a pair of parallel, independently actuated rollers that are positioned above the bed. The rollers are positioned using rods or arms that may be moved in two-dimensional vertical planes. In general, the structure may either be part of the bed itself or may form a separate portable system. In the prototype used for implementation of our control scheme, the structure is part of the bed frame. Each end of a bedsheet is attached to a roller using *Velcro*$^{TM}$. The arms are actuated

(with motors) at $O_1$ and $O_2$ and the rollers at $R_1$ and $R_2$. The system has four degrees of freedom, the rotation of the arms, $\theta_1$ and $\theta_2$ , and the rotation of the rollers, $\gamma_1$ and $\gamma_2$.

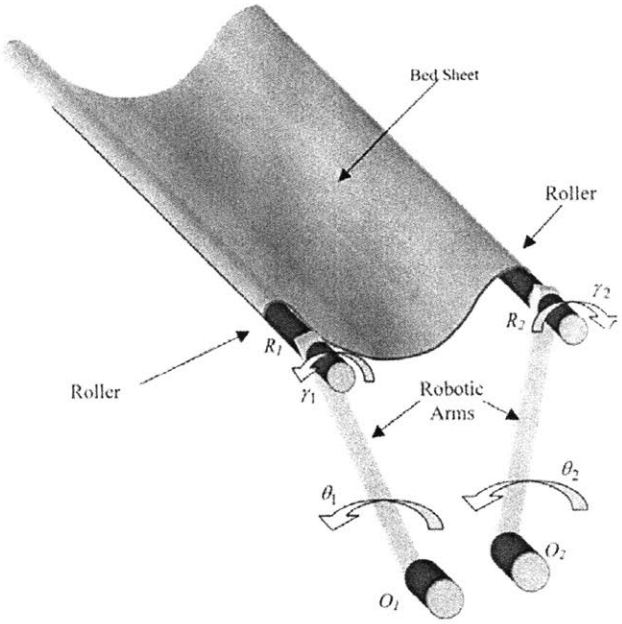


**Fig. 1.3. Schematic of Design**

Fig. 1.4 shows a picture of the prototype bed with a dummy patient lying on it. The arms and the rollers shown in the picture are actuated as mentioned above. The arms move in a circular trajectory and the rollers mounted on the arms wind or unwind the bed sheet as demanded by the maneuvering operation. Thus the patient is completely cradled by the bed sheet during the movement, much like the actual repositioning operation performed by the caregivers. Moreover, if the patient is lifted clear of the bed sheet during repositioning, she is also free from the influence of harmful shear forces which could cause/aggravate bedsores.

**Fig. 1.4. Prototype bed with dummy patient**

In this thesis, we first examine the key features of the interaction of a rigid body with a flexible bed sheet and then proceed to model and analyze the system. Subsequently, we develop a kinematic model of the prototype bed. These models are used along with sensor feedback to coordinate the motions of multiple actuators so as to position and orient the patient in a desired fashion. The patient position and orientation is sensed using a suitable sensor and is fed back to the actuators to ensure safe closed loop control. The details of the implementation scheme are discussed in Chapter 3. Chapter 4 concludes this work by listing a summary of the important results that have been derived and recommends improvements to the existing device.

# Chapter 2
# SYSTEM MODELING AND ANALYSIS

## 2.1 Objectives of Modeling and Analysis

Fig. 2.1 shows a cross sectional view of the generic configuration of our system. The body is not securely connected to the flexible sheet. At any instant, the sheet is in contact with the body over the region $B_1B_2$ (assuming a convex cross section) and the contact extremities $B_1$ and $B_2$ keep changing relative to the body. In order to coordinate the motions of the four actuators to position and the orient the body as desired, we must first determine the changing contact extremities as a function of the position and orientation of the body.

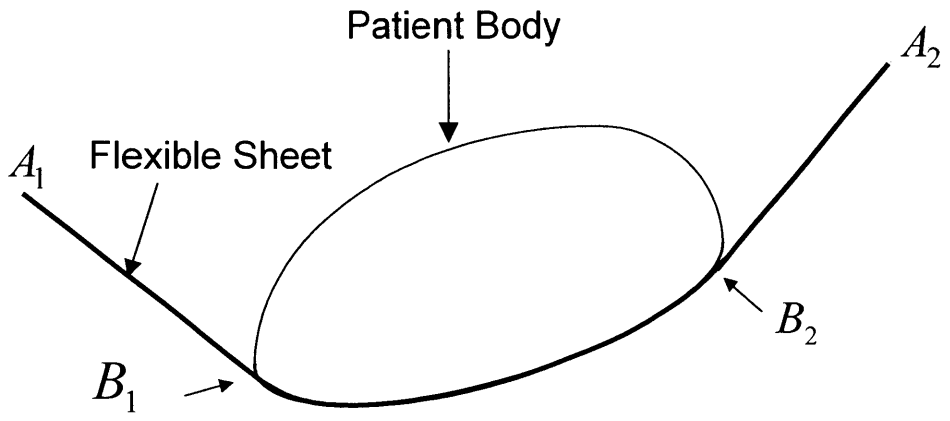


**Fig. 2.1 Generic configuration of system**

The slippage of the patient body on the sheet is extremely dangerous and is likely to damage the fragile skin of bedridden patients. Thus we must devise a criterion to ensure that there is no slippage between the body and the sheet during the repositioning operation.

We make the following assumptions in our analysis:

i. No elongation of sheets

The sheet is considered to be inelastic. Cotton sheets were used in the experiments and they did not undergo any significant elongation during the operation of the bed.

ii. Quasi-static Equilibrium

The body is assumed to be in quasi-static equilibrium. The safety and comfort of the patient is very important during the repositioning operation. All tasks are thus performed sufficiently slowly and this assumption is valid.

### *A. Free-Body Diagram*

The static behavior of a rigid body suspended with a sheet is analyzed in this section. Fig. 2.2 shows a cross-sectional view of the rigid body suspended by a sheet, in a vertical plane perpendicular to the length of the sheet. The tensions in the two straight segments of the sheet are denoted by $\mathbf{T_1}$ and $\mathbf{T_2}$. The cross-section of the real human body is complex and unpredictable, varying from the head to the feet. Accordingly, the tension of the bed sheet varies and is distributed over the bed sheet surface. The tension $\mathbf{T_1}$ ( $\mathbf{T_2}$) in the figure is the total tension aggregated over the bed sheet on the left (right) hand side of the body.

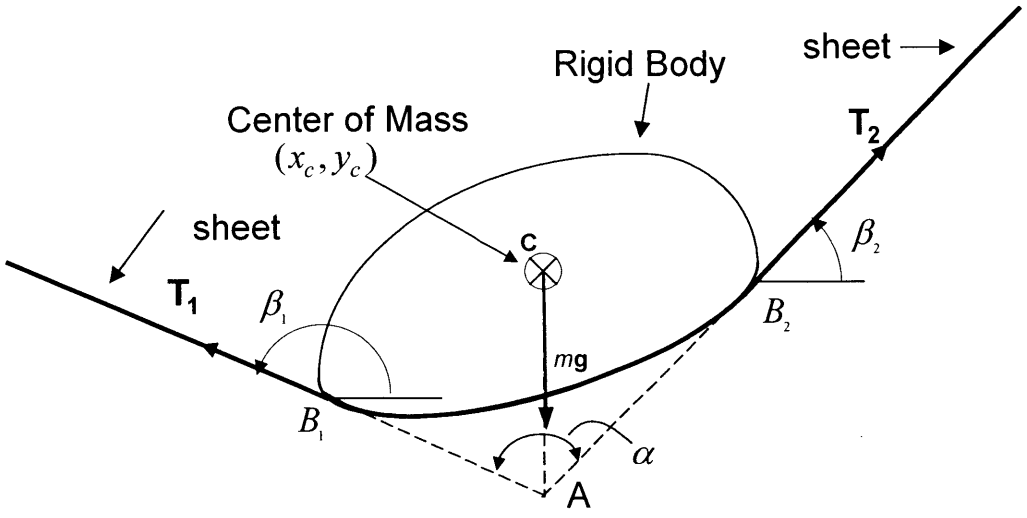


**Fig. 2.2. Free-body diagram of suspended rigid body**

As the system is in equilibrium, the line of action of the gravity force $m\mathbf{g}$ and the lines of action of the tensions $\mathbf{T_1}$ and $\mathbf{T_2}$ intersect at the same point, as shown by point $A$ in Fig. 2.2. The magnitudes of the sheet tensions $\mathbf{T_1}$ and $\mathbf{T_2}$ can be calculated using a force balance.

$$T_1 \cos\beta_1 + T_2 \cos\beta_2 = 0 \tag{2.1}$$

$$T_1 \sin\beta_1 + T_2 \sin\beta_2 = mg \tag{2.2}$$

Solving (2.1) and (2.2) for $T_1$ and $T_2$ yield:

$$T_1 = \frac{\cos\beta_2}{\sin(\beta_1 - \beta_2)} mg = \frac{\cos\beta_2}{\sin\alpha} mg \tag{2.3}$$

$$T_2 = -\frac{\cos\beta_1}{\sin(\beta_1 - \beta_2)} mg = -\frac{\cos\beta_1}{\sin\alpha} mg \tag{2.4}$$

We have written the equilibrium equations by considering the system (body and sheet) as a whole. However, it must be noted that the contact forces of friction and normal

reaction govern the equilibrium of the body and the sheet taken individually. Hence, the equilibrium position is valid only when there is sufficient friction to prevent slip.

### *B. Friction Force Analysis*

In this section, we derive a relationship between the angle of inclination of the body with the horizontal *($\phi$)*, the angle between the straight segments of the sheet *($\alpha$)*, the coefficient of static friction ($\mu$) and the shape of the body. We do this by first relating the body shape and the friction coefficient to the angles $\beta_1$ and $\beta_2$ and then we substitute for these angles in terms of $\phi$ and $\alpha$.

In the analysis that follows, it is assumed that the cross section of the rigid body is uniform. Fig. 2.3 shows a differential element *ds* of the sheet and its free-body diagram. The sheet element subtends an angle $d\xi$ at its center of curvature $C$ and the radius of curvature is $r$. The forces acting on the sheet element are the normal reaction **dN**, the friction force **df** and the sheet tensions **T** and **T+dT**.

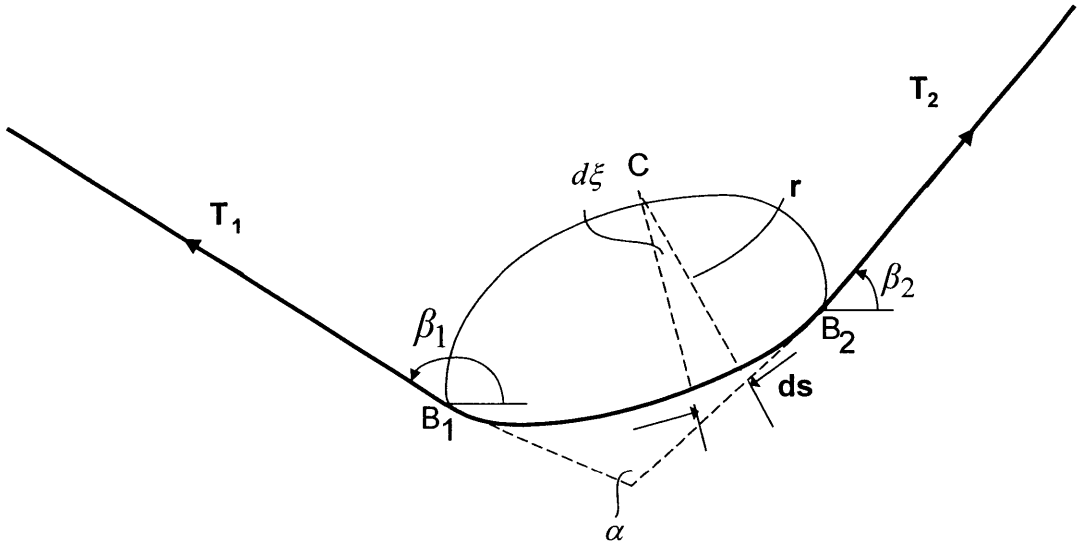

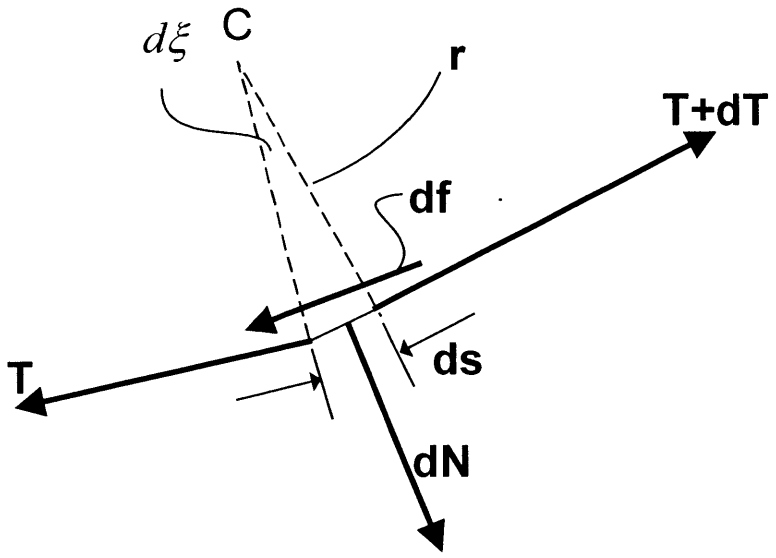


**Fig. 2.3. Free body diagram of sheet element**

Considering the equilibrium of the differential segment *ds* of the sheet in the tangential and normal directions, we may write:

$$df = (T + dT)\cos\frac{d\xi}{2} - T\cos\frac{d\xi}{2} = dT \tag{2.5}$$

$$dN = (T + dT)\sin\frac{d\xi}{2} + T\sin\frac{d\xi}{2} = Td\xi = T\frac{ds}{r} \tag{2.6}$$

The relationship between the friction force and the normal reaction is given by:

$$df \leq \mu dN \tag{2.7}$$

where $\mu$ is the coefficient of static friction. The inequality is strict as long as the body is not slipping on the sheet and equality holds at incipient slip. Substituting *df* from (2.5) and *dN* from (2.6) into (2.7), we get:

$$dT \leq \mu T\frac{ds}{r} \tag{2.8}$$

$$\therefore \quad \frac{dT}{T} \leq \mu \frac{ds}{r} \tag{2.9}$$

We may now integrate the above equation from one contact extremity to the other ($B_1$ to $B_2$) to get:

$$\ln \frac{T_2}{T_1} \leq \int_{B_1}^{B_2} \mu \frac{ds}{r} \tag{2.10}$$

Using (2.3) and (2.4), (2.10) can be written as:

$$\ln \frac{-\cos \beta_1}{\cos \beta_2} \leq \int_{B_1}^{B_2} \mu \frac{ds}{r} \tag{2.11}$$

The relationship in (2.11) represents the criterion for no slip to occur as a function of the friction coefficient, the body shape and the angles $\beta_1$ and $\beta_2$. The right hand side of (2.11) can be evaluated if the body shape is known. A necessary condition for the integral to be evaluated is that the bounding curve of the cross section be continuously differentiable. If the body cross section is convex throughout, then the sheet is in contact with the body along the whole arc $B_1B_2$. If the cross section is concave in parts, the sheet is in contact only along the convex parts of the cross section between $B_1$ and $B_2$. In that case, the tension of the sheet remains constant in the concave regions (as it is not in contact) and the integral in (2.11) must be evaluated only in the convex regime.

### *C. Special Case: An elliptical Cylinder*

We investigate (2.11) more closely by assuming a specific body shape and evaluating the integral. In the analysis that follows, we assume that the rigid body is shaped as an elliptical cylinder. However, it is emphasized that the methodology is perfectly general

and can be extended to any cross section, which satisfies the conditions mentioned in the derivation of (2.11).

Our first task is to determine the changing contact extremities as a function of the orientation of the body and the angle between the two straight segments of the sheet.

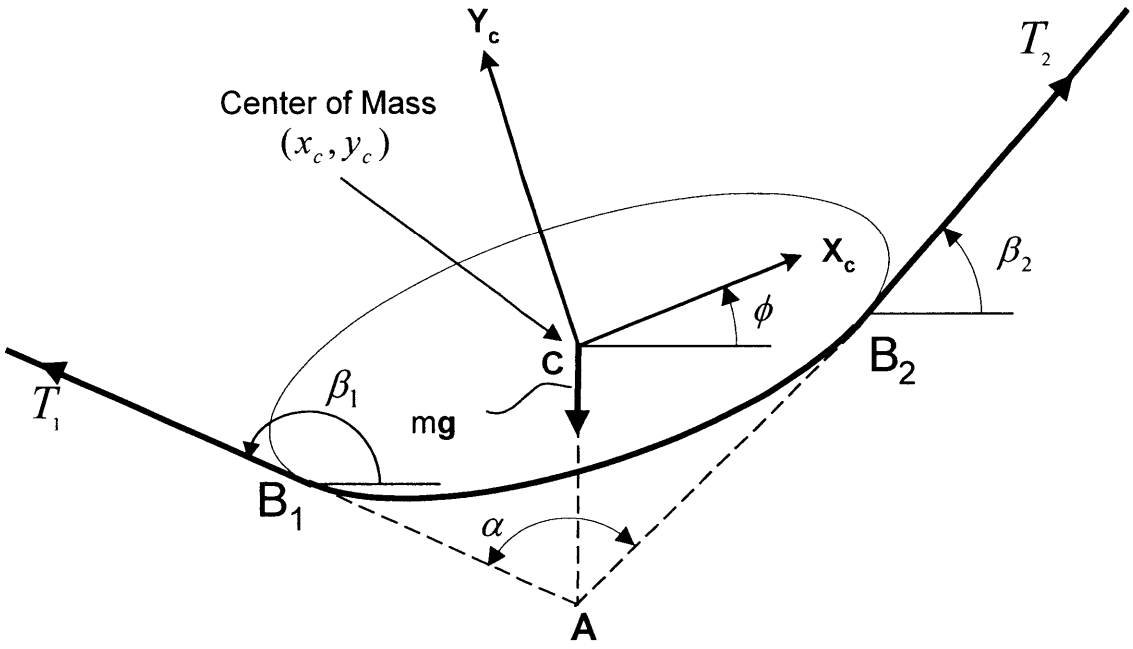


**Fig. 2.4. Elliptical Cylinder suspended by sheet**

Fig. 2.4 shows a cross sectional view of the elliptical cylinder on the sheet. Let ***C*-$\mathbf{X_cY_c}$** be a frame fixed to the center of mass of the body and aligned with the major axis of the ellipse. The primed parameters and coordinates are referenced to the body coordinate system and the unprimed ones are referenced to the world coordinate system. Let $\psi_i'$ be the eccentric angle of point $B_i$ on the ellipse. The coordinates of any point P on the ellipse may be parameterized in terms of the eccentric angle as

$$x' = a\cos\psi' \ , \ y' = b\sin\psi' \tag{2.12}$$

From the geometry of the problem, the straight segments of the sheet are tangent to the cross section at the contact extremities. The equations of the tangents are given by:

$$\frac{x'}{a} + \frac{y'\tan\psi_1'}{b} - \sec\psi_1' = 0 \tag{2.13}$$

$$\frac{x'}{a} + \frac{y'\tan\psi_2'}{b} - \sec\psi_2' = 0 \tag{2.14}$$

Let $\alpha$ be the angle between the two tangents:

$$\alpha = \beta_1 - \beta_2 = (\beta_1 - \phi) - (\beta_2 - \phi) \tag{2.15}$$

From (2.13) and (2.14), the slopes of the tangents are given by:

$$m_1' = \frac{-b\cot\psi_1'}{a} = \tan(\beta_1 - \phi) \tag{2.16}$$

$$m_2' = \frac{-b\cot\psi_2'}{a} = \tan(\beta_2 - \phi) \tag{2.17}$$

From (2.15), (2.16) and (2.17) we get:

$$\tan\alpha = \frac{m_1' - m_2'}{1 + m_1' m_2'} = \frac{b(\tan\psi_1' - \tan\psi_2')}{a(\tan\psi_1'\tan\psi_2' + \frac{b^2}{a^2})} \tag{2.18}$$

Solving (2.13) and (2.14) for the point of intersection, $A$, of the tangents, we get:

$$x_A' = \frac{a(\sec\psi_2'\tan\psi_1' - \sec\psi_1'\tan\psi_2')}{\tan\psi_1' - \tan\psi_2'} \tag{2.19}$$

$$y_A' = \frac{b(\sec\psi_1' - \sec\psi_2')}{\tan\psi_1' - \tan\psi_2'} \tag{2.20}$$

When the body is fully suspended and clear of the bed mattress, i.e. airborne, the line of action of the gravity force ***mg*** and the lines of action of the tensions $T_1$ and $T_2$ intersect at the same point, as shown by point $A$ in the figure. Thus:

$$\frac{y'_A}{x'_A} = \cot\phi \tag{2.21}$$

From (2.19) and (2.20) this can be rewritten as:

$$\cot\phi = \frac{b(\sec\psi'_1 - \sec\psi'_2)}{a(\sec\psi'_2 \tan\psi'_1 - \sec\psi'_1 \tan\psi'_2)}$$

$$= \frac{b\tan(\frac{\psi'_1 + \psi'_2}{2})}{a} \tag{2.22}$$

Equations (2.18) and (2.22) represent the relationships between the coordinates ($\psi'_1$ and $\psi'_2$) of the contact extremities ($B_1$ and $B_2$) and the angles $\phi$ and $\alpha$. We wish to obtain closed form solutions for $\psi'_1$ and $\psi'_2$ in terms of $\phi$ and $\alpha$. We introduce the following notation:

$$x = \tan\psi'_1, y = \tan\psi'_2 \tag{2.23}$$

Using the above notation, (2.18) may be rewritten as:

$$\frac{x - y}{\frac{1}{K} + xy} = M \tag{2.24}$$

where:

$$M = \frac{a\tan\alpha}{b} \tag{2.25}$$

$$K = \frac{a^2}{b^2} \tag{2.26}$$

Using $\tan 2\theta = \dfrac{2\tan\theta}{1-\tan^2\theta}$, from (2.22) we get:

$$\tan(\psi_1' + \psi_2') = \frac{\tan\psi_1' + \tan\psi_2'}{1-\tan\psi_1'\tan\psi_2'} = \frac{2\dfrac{a}{b}\cot\phi}{1-\dfrac{a^2}{b^2}\cot^2\phi} \tag{2.27}$$

We rewrite (2.27) in the revised notation to get:

$$\frac{x+y}{1-xy} = L \tag{2.28}$$

where:

$$L = \frac{2\dfrac{a}{b}\cot\phi}{1-\dfrac{a^2}{b^2}\cot^2\phi} \tag{2.29}$$

We can now solve (2.24) and (2.28) simultaneously, for $x$ and $y$, to obtain:

$$x = \frac{-B \pm \sqrt{B^2 - 4AC}}{2A} \tag{2.30}$$

where:

$$A = L + M \tag{2.31}$$

$$B = 2 - LM\left(1 + \frac{1}{K}\right) \tag{2.32}$$

$$C = -L - \frac{M}{K} \tag{2.33}$$

Also,

$$y = \frac{x - \dfrac{M}{K}}{1 + Mx} \tag{2.34}$$

It is also useful to determine $\beta_1$ and $\beta_2$ as functions of $\phi$ and $\alpha$. From (2.16), using the notation in (2.23), we may solve for $\beta_1$. Thus:

$$\tan\beta_1 = \frac{\frac{a}{b}x\tan\phi - 1}{\tan\phi + \frac{a}{b}x} \tag{2.35}$$

Similarly, from (2.17), using the notation in (2.23), we may write:

$$\tan\beta_2 = \frac{\frac{a}{b}y\tan\phi - 1}{\tan\phi + \frac{a}{b}y} \tag{2.36}$$

Having determined the contact extremities as well as the angles $\beta_1$ and $\beta_2$ as functions of $\phi$ and $\alpha$, we can evaluate the integral on the right hand side of (11). It is useful to parameterize the quantities involved in the integral in terms of the eccentric angle ($\psi'$) of a point on the ellipse.

The general expression for arc length of a parametric curve is given by:

$$ds = \sqrt{(\frac{dx'}{d\psi'})^2 + (\frac{dy'}{d\psi'})^2}\, d\psi' \tag{2.37}$$

In the special case of the ellipse, using (2.12), this reduces to:

$$\begin{aligned} ds &= \sqrt{a^2\sin^2\psi' + b^2\cos^2\psi'}\, d\psi' \\ &= \frac{b\sqrt{\frac{a^2}{b^2}\tan^2\psi' + 1}}{\sec\psi'} d\psi' \end{aligned} \tag{2.38}$$

By definition, the radius of curvature at any point of a parameterized curve is given by:

$$r = \frac{[(\frac{dx'}{d\psi'})^2 + (\frac{dy'}{d\psi'})^2]^{\frac{3}{2}}}{\frac{dx'}{d\psi'}\frac{d^2y'}{d\psi'^2} - \frac{dy'}{d\psi'}\frac{d^2x'}{d\psi'^2}} \tag{2.39}$$

In our case (2.39) reduces to:

$$r = \frac{(a^2 \sin^2 \psi' + b^2 \cos^2 \psi')^{\frac{3}{2}}}{ab} = \frac{b^2 (\frac{a^2}{b^2} \tan^2 \psi' + 1)^{\frac{3}{2}}}{a \sec^3 \psi'} \tag{2.40}$$

Using (2.38) and (2.40), (2.11) can be rewritten as:

$$\ln \frac{-\cos \beta_1}{\cos \beta_2} \leq \int_{\psi_1'}^{\psi_2'} \frac{\mu K^{\frac{1}{2}} \sec^2 \psi' d\psi'}{K \tan^2 \psi' + 1} \tag{2.41}$$

We evaluate this integral by introducing the substitution:

$$t = \tan \psi' \tag{2.42}$$

Using (2.23) and (2.42), the relationship in (2.41) may then be rewritten in the form:

$$\ln \frac{1 + \tan^2 \beta_2}{1 + \tan^2 \beta_1} \leq 2\mu K^{\frac{1}{2}} \int_x^y \frac{dt}{Kt^2 + 1} \tag{2.43}$$

The integral in (2.43) permits a closed form solution and the relationship can be simplified to:

$$\ln \frac{1 + \tan^2 \beta_2}{1 + \tan^2 \beta_1} \leq 2\mu [\tan^{-1}(K^{\frac{1}{2}} y) - \tan^{-1}(K^{\frac{1}{2}} x)] = 2\mu \tan^{-1} \frac{K^{\frac{1}{2}}(y - x)}{1 + Kxy} \tag{2.44}$$

It is to be noted that the inverse tangent is evaluated in the range $[0,\pi]$.

We use (2.35) and (2.36) in the LHS of (2.44) to obtain an implicit inequality involving $\phi$, $\alpha$ and $\mu$. A closed form relationship between $\phi$ and $\alpha$ cannot be obtained. However, (2.44) can be solved numerically to yield the maximum permissible $\alpha$ before slip occurs for a particular value of $\phi$, given the aspect ratio $k$ and the coefficient of friction $\mu$. Fig.

2.5 shows a plot of the results for an aspect ratio of 2.9 and the coefficient of friction increasing in the direction of the arrow from 0.1 to 0.9. The region below each line represents the range of $\alpha$ for no slip for the particular coefficient of friction and angle of inclination. Mathematically, the points on each line represent the critical value of $\alpha$ at

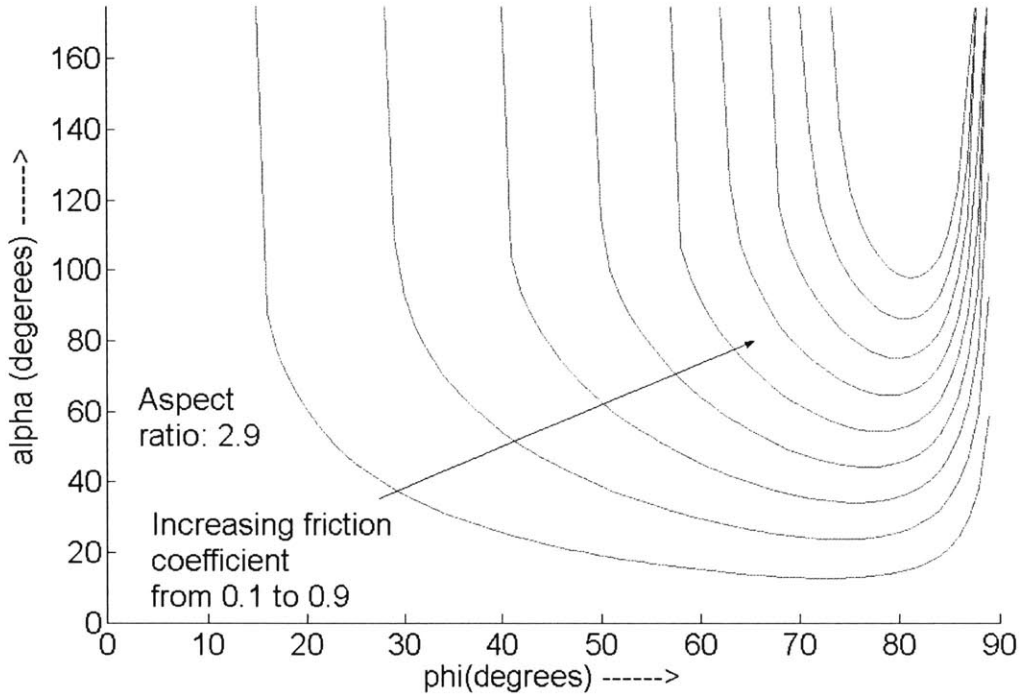


**Fig. 2.5. Maximum permissible α before slip**

which the inequality is violated, for a particular value of $\phi$ and the coefficient of friction corresponding to that line. When the angle of inclination of the body with the horizontal is small, a value of $\alpha$ close to 180° is permissible. This corresponds to the stable horizontal equilibrium position when friction has little effect. We also observe that the value of $\alpha$ rises significantly to about 180° when the angle of inclination of the body is close to 90°. This corresponds to the unstable vertical equilibrium position.

We now compare the theoretical prediction based on the above model with experimental data. Experiments were conducted using an elliptical cylinder with an aspect ratio of 2.9, and the value of $\alpha$ for which slip occurred for a particular value of $\phi$ was noted. The actual setup was such that the value of $\alpha$ was incremented in steps and the value of $\phi$ for which the elliptical cylinder started slipping was noted. The value of $\alpha$ was controlled using the closed loop control strategy described in Chapter 4. The following experiment was conducted to estimate the coefficient of friction. A sample of the bed sheet was stretched flat on a hard surface and the elliptical cylinder was placed on it. The cylinder was then pushed using a stick with a force sensor attached to its tip and the force at which the cylinder started slipping was recorded. The force at which the body starts to slip, when divided by the normal reaction (the weight of the cylinder in this case), gives an estimate for the coefficient of static friction. The coefficient of friction between the bed sheet and the elliptical cylinder was experimentally determined to be 0.2. Fig. 2.6 shows the superimposed plots of the theoretical and experimental data. A second degree polynomial was fitted to the experimental data using the least squares technique. The fitted polynomial was (all angles in degrees):

$$\alpha = .0707\phi^2 - 7.8558\phi + 258.7226 \tag{2.45}$$

The experimental results show a close agreement with the theoretical model and leads us to believe that the theoretical model is a reasonable description of the physical situation. The discrepencies between the theoretical model and the experimental data may also be partly attributed to the nature of the "measurement" of $\alpha$. As described in Chapter 4, the value of $\alpha$ used is actually an estimate (approximate calculated value) based on other sensor measurements (motor encoder and body position and orientation), rather

than a direct measurement. Thus, the theoretical model can be used to determine the range of $\alpha$ for no slip of the patient on the sheet for a given value of $\phi$ and an estimated coefficient of friction. The slippage is a serious concern for the fragile skin of a bedridden patient and it is thus advisable to use the theoretical estimate with a reasonable factor of safety (say 1.5 to 2) in an actual hospital scenario.

The angle $\alpha$ might have seemed superfluous at first glance, since we were only trying to position and orient the patient. However, from the analysis above, the role of the angle $\alpha$ is now clear. It is no longer a free variable that can be chosen independently for the task at hand. Rather, the value of $\alpha$ must be restricted to a certain range for the successful implementaion of the task. This once again justifies the use of four actuators (motors) to control the four degees of freedom of the patient-sheet system.

| **α:** *Angle between straight segments of sheet* **(degrees)** | **ϕ:** *Maximum inclination with horizontal before slip* **(degrees)** |
|---|---|
| 40 | 53 |
| 45 | 50 |
| 50 | 43 |
| 55 | 40 |
| 60 | 39 |
| 65 | 37 |
| 70 | 36 |
| 75 | 34 |

| | |
|---|---|
| 80 | 32 |
| 85 | 30 |

**Table 2.1. Experimental data relating $\alpha$ and $\phi$ at impending slippage**

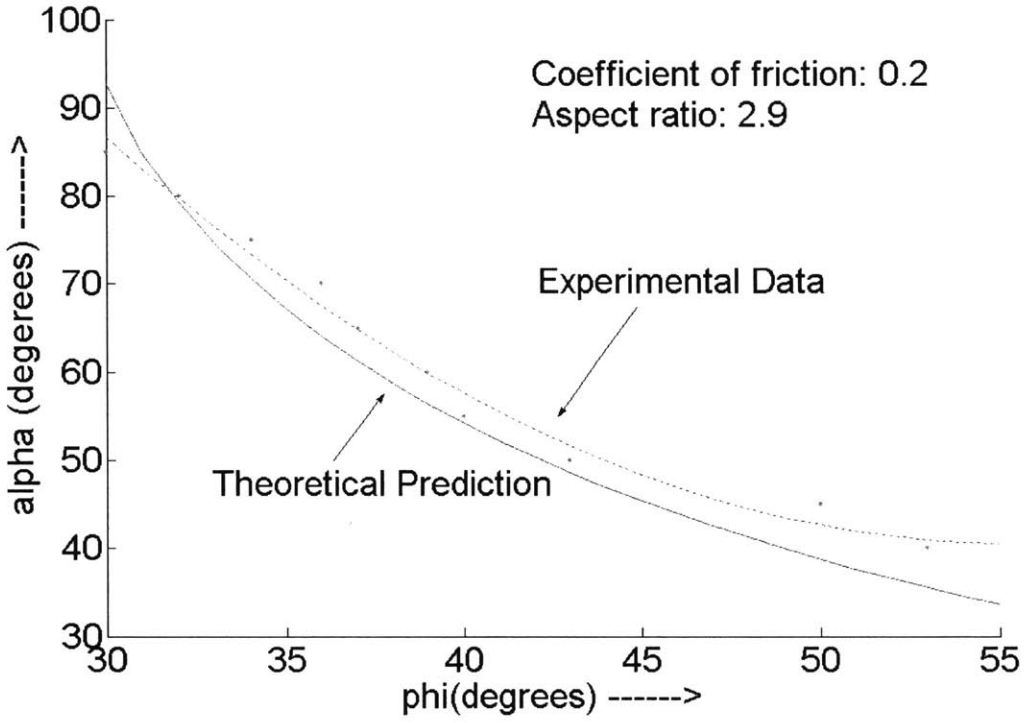


**Fig. 2.6. Comparison of experimental data and theoretical prediction**

It is interesting to analyze the equilibria of an elliptical cylinder for the case where friction is absent. It turns out that even in the absence of friction, it is possible to orient the cylinder at an arbitrary angle to the horizontal. However, the angle $\alpha$ cannot be chosen arbitrarily.

In the absence of friction the tension must be the same along the contact length. The moments of the tensions about the center of mass must also balance. Thus the perpendicular distance from the center of mass to the lines of actions of the tensions must

be the same. In other words, the contact extremities of the sheet and the body must be symmetric with respect to the major/minor axis of the ellipse or with respect to the center. With reference to Fig. 2.7, let us first consider the case:

$$d > 2a$$

Since, the contact extremities are symmetric, the lines of action of the two tensions must meet on the major/minor axis extended. Furthermore, from equilibrium, the lines of action of the two tensions and gravity must be concurrent. Hence, we may conclude that the horizontal and the vertical positions are the only equilibrium positions. The horizontal position is stable and the vertical position is unstable.

Next, let us consider the case:

$$d < 2b$$

Following the arguments above, we may once again conclude that the horizontal and the vertical positions are the only equilibrium positions. The horizontal position is stable and the vertical position is unstable.

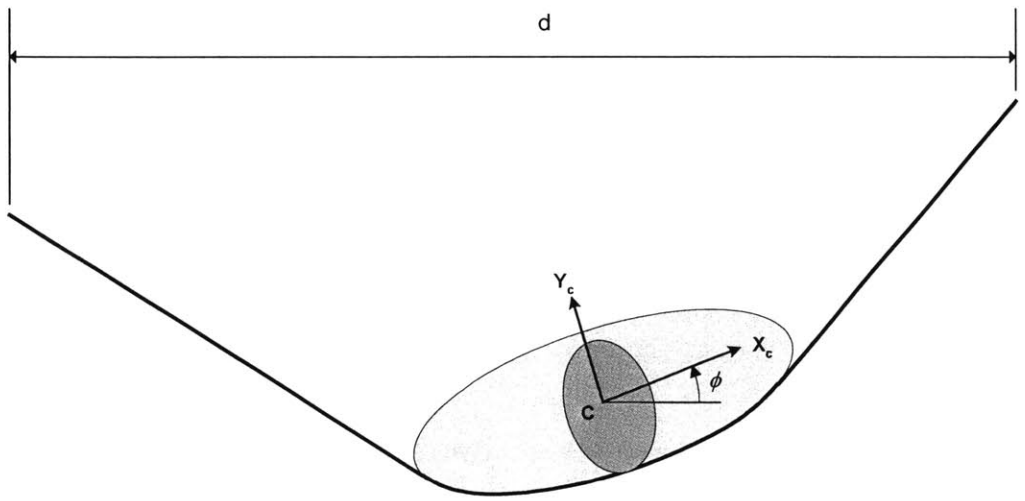

**Fig. 2.7. Body suspended by sheet (frictionless case)**

The last case that we consider is:

$$2b < d < 2a$$

In this case, in addition to the horizontal and vertical positions, there are two other equilibrium positions given by:

$$\cos\phi = \pm\frac{1}{2}\sqrt{\frac{d^2 - 4b^2}{a^2 - b^2}} \tag{2.46}$$

For these values of $\phi$ the line of action of the tensions are vertical. Thus, by choosing $d$ suitably, it is possible to align the body at an arbitrary angle to the horizontal.

### *D. Kinematics of Robotic Arms*

Now that the no-slip condition has been established, we will describe a strategy for coordinating the motions of the robotic arms and the mounted rollers in order to reposition the human body. Let us consider two fixed points, **L** and **R**, on the bedsheet, on either side of the body, as shown in Fig. 2.8. To control the body position and inclination, we must be able to move the points **L** and **R** to arbitrary positions within the two-dimensional vertical plane. This may be performed by a pair of two degree-of-freedom robotic arms, each holding **L** and **R**. An alternative to such a design is to combine one degree-of-freedom arms with powered rollers that wind up the bedsheet.

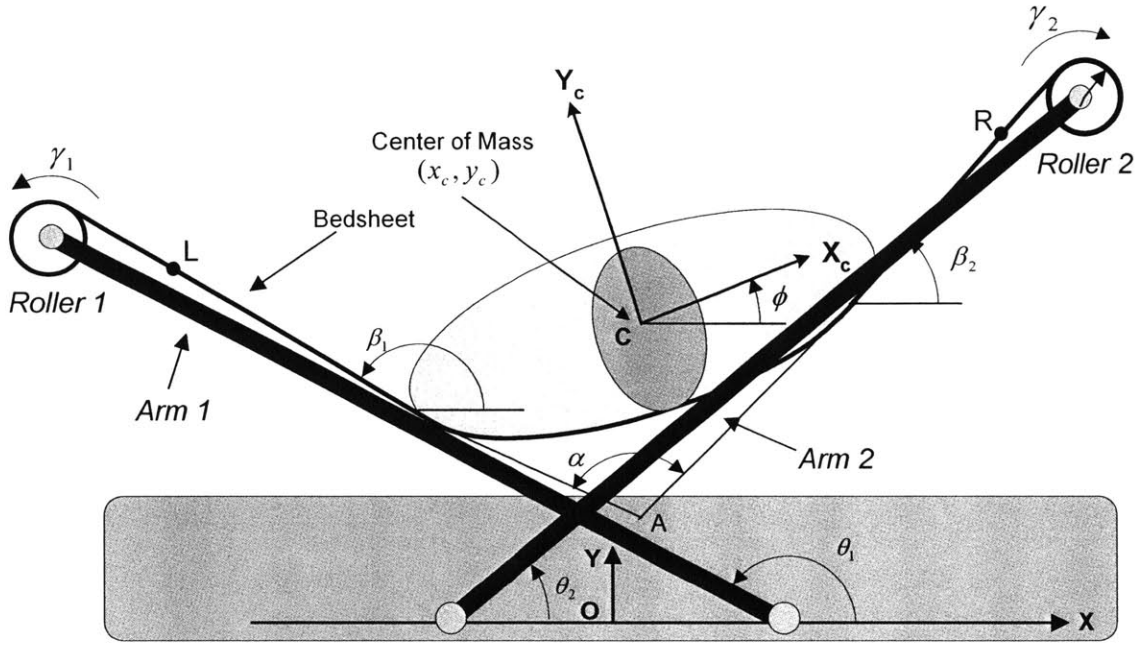


**Fig. 2.8. Schematic of a suspended human body on the rehabilitation bed**

Fig. 2.8 shows the kinematic configuration of a pair of one d.o.f. arms with powered rollers. Let $\theta_i$ ($i$=1,2) be the joint angle of the arm and let $\gamma_i$ be the roller rotation relative to the arm. Let $(x_c, y_c)$ be the coordinates of the center of mass of the body and $\phi$ the angle of inclination of the body with the horizontal.. Let $\mathbf{q} \in R^{4\times1}$ be the actuator coordinates representing the displacements (rotations) of the four actuators, and $\mathbf{p} \in R^{4\times1}$ be the resultant body position and orientation along with the angle between the straight segments of the sheet. The vector **q** describes the inputs to the system while the vector **p** describes the variables or outputs to be controlled. Thus:

$$\mathbf{p} = [x_c \;\; y_c \;\; \phi \;\; \alpha]^T \tag{2.47}$$

$$\mathbf{q} = [\theta_1 \;\; \theta_2 \;\; \gamma_1 \;\; \gamma_2]^T \tag{2.48}$$

Our task is to determine the components of **q** as functions of the components of **p**. We first determine the angles $\theta_1$ and $\theta_2$ and then proceed to determine $\gamma_1$ and $\gamma_2$. Fig. 2.9 shows the body suspended on the sheet but the robotic arms have been removed for clarity.

From Fig. 2.9:

$$\vec{\mathbf{OC}}+\vec{\mathbf{CB}}_2=\vec{\mathbf{OB}}_2=\vec{\mathbf{OM}}_2+\vec{\mathbf{M}_2\mathbf{R}_2}+\vec{\mathbf{R}_2\mathbf{E}_2}+\vec{\mathbf{E}_2\mathbf{B}_2} \tag{2.49}$$

The vector relationship (2.49) may be written in component form to yield the 2 scalar equations:

$$\begin{aligned} &x_c+a\cos\psi_2'\cos\phi-b\sin\psi_2'\sin\phi \\ &=-D-r_2\sin\beta_2+l_2\cos\theta_2-L_2\cos\beta_2 \end{aligned} \tag{2.50}$$

$$\begin{aligned} &y_c+a\cos\psi_2'\sin\phi+b\sin\psi_2'\cos\phi \\ &=l_2\sin\theta_2+r_2\cos\beta_2-L_2\sin\beta_2 \end{aligned} \tag{2.51}$$

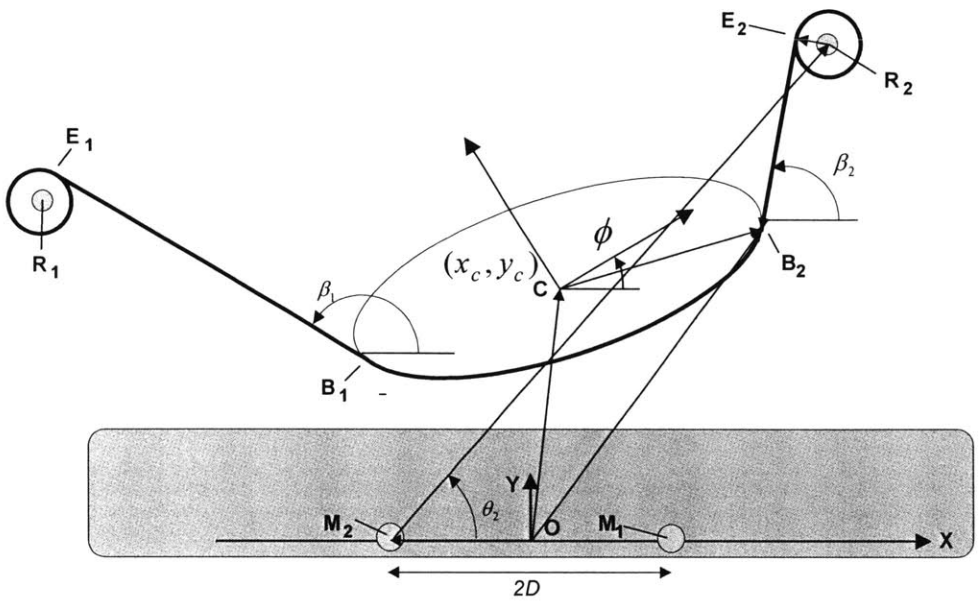


**Fig. 2.9. Position vector of contact extremity**

where $D$ is the distance of the arms' revolute joints from the coordinate origin $O$ and $L_2$ is the length $B_2E_2$. Also, $r_2$ is the radius of the roller and $l_2$ is the length of the arm $M_2R_2$. Solving these equations for joint angle $\theta_2$ yields:

$$\cos\theta_2 = \frac{b_2 c_2 \pm \sqrt{b_2^2 - c_2^2 + 1}}{b_2^2 + 1} \tag{2.52}$$

where

$$b_2 = -\tan\beta_2 \tag{2.53}$$

$$\begin{aligned} c_2 = (&y_c - r_2\cos\beta_2 + b\sin\psi_2'\cos\phi + a\cos\psi_2'\sin\phi \\ &+ \tan\beta_2(-D - r_2\sin\beta_2 - x_c - a\cos\psi_2'\cos\phi + b\sin\psi_2'\sin\phi))/l_2 \end{aligned} \tag{2.54}$$

Similarly, we may calculate the joint angle $\theta_1$.

We use a velocity constraint between the body and the sheet to calculate $\gamma_i$ in terms of the outputs. Let us consider two points, fixed to the sheet. One of the points is at $B_i$ and the other is at $E_i$ at the instant shown in Fig. 2.9. Since the sheet is taut and assumed to be

inextensible, the component of the relative velocity of two points $B_i$ and $E_i$, along the line joining them, must be zero. In the following equations the superscript $t$ refers to the tangential component (tangent to the solid surface at the point of contact) of the velocity. Hence:

$$(v_{B_i}^t)_{sheet} = (v_{E_i}^t)_{sheet} \tag{2.55}$$

Furthermore, if $\alpha$ is chosen so that there is no slip between the body and the sheet, we have:

$$(v_{B_i}^t)_{body} = (v_{B_i}^t)_{sheet} \tag{2.56}$$

In the above equation, the left hand side refers to the velocity of a point on the body, which is instantaneously coincident with the point $B_i$ on the sheet. Similarly for the roller:

$$(v_{E_i}^t)_{sheet} = (v_{E_i}^t)_{roller} \tag{2.57}$$

Once again, the right hand side refers to the velocity of a point on the roller, which is instantaneously coincident with the point $E_i$ on the sheet. From (2.55), (2.56) and (2.57) we conclude:

$$(v_{B_i}^t)_{body} = (v_{E_i}^t)_{roller} \tag{2.58}$$

For the point $B_i$ on the body, we may write:

$$\mathbf{v}_{B_i} = \mathbf{v}_C + \boldsymbol{\omega}_{body} \times \mathbf{CB}_i \tag{2.59}$$

We rewrite the tangential component of (2.59) for $i$=1,2 in scalar form as:

$$v_{B_1}^t = -\dot{x}_c \cos\beta_1 - \dot{y}_c \sin\beta_1 - \rho_1 \dot{\phi} \sin(\beta_1 - \varepsilon_1) \tag{2.60}$$

$$v_{B_2}^t = \dot{x}_c \cos\beta_2 + \dot{y}_c \sin\beta_2 + \rho_2 \dot{\phi} \sin(\beta_2 - \varepsilon_2) \tag{2.61}$$

Similarly, for the point $E_i$ on the roller, we may write:

$$\mathbf{v}_{E_i} = \mathbf{v}_{R_i} + \boldsymbol{\omega}_{roller} \times \mathbf{R}_i\mathbf{E}_i \tag{2.62}$$

We rewrite the tangential component of (39) for $i$=1,2 in scalar form as:

$$v^t_{E_1} = l_1 \dot{\theta}_1 \sin(\theta_1 - \beta_1) - r_1(\dot{\theta}_1 + \dot{\gamma}_1) \tag{2.63}$$

$$v^t_{E_2} = -l_2 \dot{\theta}_2 \sin(\theta_2 - \beta_2) - r_2(\dot{\theta}_2 - \dot{\gamma}_2) \tag{2.64}$$

Using (2.58), (2.60) and (2.63) we may write:

$$l_1\dot{\theta}_1 \sin(\theta_1 - \beta_1) - r_1\dot{\theta}_1 + \dot{x}_c \cos\beta_1 + \dot{y}_c \sin\beta_1 + \rho_1\dot{\phi}\sin(\beta_1 - \varepsilon_1) = r_1\dot{\gamma}_1 \tag{2.65}$$

Similarly, from (2.58), (2.61) and (2.64), we may write:

$$l_2\dot{\theta}_2 \sin(\theta_2 - \beta_2) + r_2\dot{\theta}_2 + \dot{x}_c \cos\beta_2 + \dot{y}_c \sin\beta_2 + \rho_2\dot{\phi}\sin(\beta_2 - \varepsilon_2) = r_2\dot{\gamma}_2 \tag{2.66}$$

where:

$$\rho_1 = \sqrt{a^2 \cos^2 \psi_1' + b^2 \sin^2 \psi_1'} \tag{2.67}$$

$$\rho_2 = \sqrt{a^2 \cos^2 \psi_2' + b^2 \sin^2 \psi_2'} \tag{2.68}$$

$$\tan\varepsilon_1 = \tan(\frac{b}{a}\tan\psi_1') \tag{2.69}$$

$$\tan\varepsilon_2 = \tan(\frac{b}{a}\tan\psi_2') \tag{2.70}$$

Equations (2.52), (2.65) and (2.66) describe the inputs required for a desired output and represent the inverse kinematics of the problem. The differential relationship between the input and the output vector is through the inverse Jacobian Matrix that can be evaluated by writing equations (2.52), (2.65) and (2.66) in differential form.

$$d\mathbf{q} = \mathbf{J}^{-1} d\mathbf{p} \tag{2.71}$$

$$\begin{bmatrix} d\theta_1 \\ d\theta_2 \\ d\gamma_1 \\ d\gamma_2 \end{bmatrix} = \begin{bmatrix} \frac{\partial\theta_1}{\partial x_c} & \frac{\partial\theta_1}{\partial y_c} & \frac{\partial\theta_1}{\partial\phi} & \frac{\partial\theta_1}{\partial\alpha} \\ \frac{\partial\theta_2}{\partial x_c} & \frac{\partial\theta_2}{\partial y_c} & \frac{\partial\theta_2}{\partial\phi} & \frac{\partial\theta_2}{\partial\alpha} \\ \frac{\partial\gamma_1}{\partial x_c} & \frac{\partial\gamma_1}{\partial y_c} & \frac{\partial\gamma_1}{\partial\phi} & \frac{\partial\gamma_1}{\partial\alpha} \\ \frac{\partial\gamma_2}{\partial x_c} & \frac{\partial\gamma_2}{\partial y_c} & \frac{\partial\gamma_2}{\partial\phi} & \frac{\partial\gamma_2}{\partial\alpha} \end{bmatrix} \begin{bmatrix} dx_c \\ dy_c \\ d\phi \\ d\alpha \end{bmatrix} \tag{2.72}$$

For the implementation of the control scheme described in the next chapter, the elements of the Jacobian matrix are evaluated numerically from the input/output equations described. This is because the analytical expressions of the derivatives involved are extremely complicated.

# Chapter 3
# IMPLEMENTATION

## 3.1 Actuator Coordination

The fundamental objective of the robotic bed is to position and orient the patient as desired. The system has 4 actuators, $M_1$, $M_2$, $M_3$ and $M_4$ as shown in Fig. 3.1. In order to perform the repositioning operation, we must coordinate the motions of the four actuators.

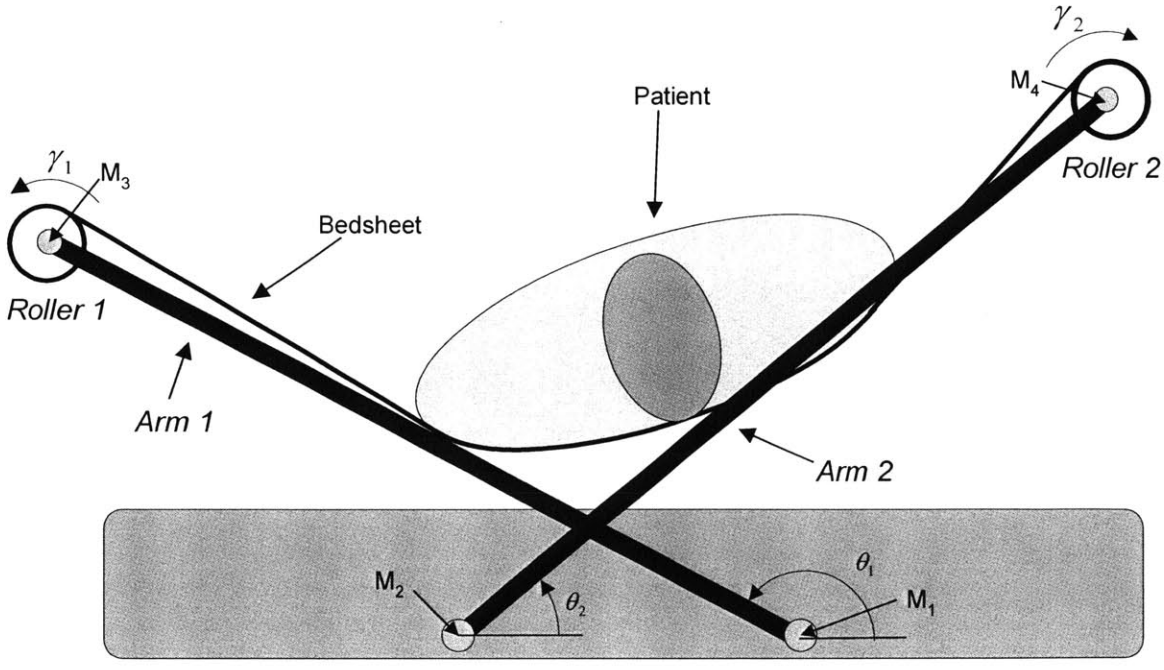


**Fig. 3.1. Schematic of patient on rehabilitation bed**

There are two levels at which the system is being controlled:

1. Generation of actuator commands to position and orient the patient.

2. Closed loop control of actuators to ensure that they follow the generated commands.

The governing relationship for the first level of control is the system Jacobian given by (38). The second level of control is accomplished by using a commercially available software package from Soft Servo Systems™. We first discuss a simple open loop control scheme at the patient level, where the actuator commands are generated using the final desired position. We then discuss a closed loop scheme using sensor feedback from the patient. The latter scheme, being closed loop, offers more accurate positioning of the patient. It is also safer because the position of the patient is being constantly monitored and the system can take corrective action if it senses that the patient is dangerously close to the edge of the bed.

### 3.1.1 Open Loop Control

As shown in the Fig. 3.2, we can use an open-loop scheme at the patient level to coordinate the motions of the actuators. Also, as shown in Fig. 3.2, the actuator control is closed loop to ensure that the actuators follow the generated commands. The desired difference in positions and orientations ($\Delta x_{cd}$, $\Delta y_{cd}$, $\Delta \phi_d$, $\Delta \alpha_d$) is fed forward to the inverse Jacobian matrix, which generates the differential angular motions of the actuators. The joint angle commands are fed to the actuator feedback control module, which ensures that the motors follow the joint angle commands.

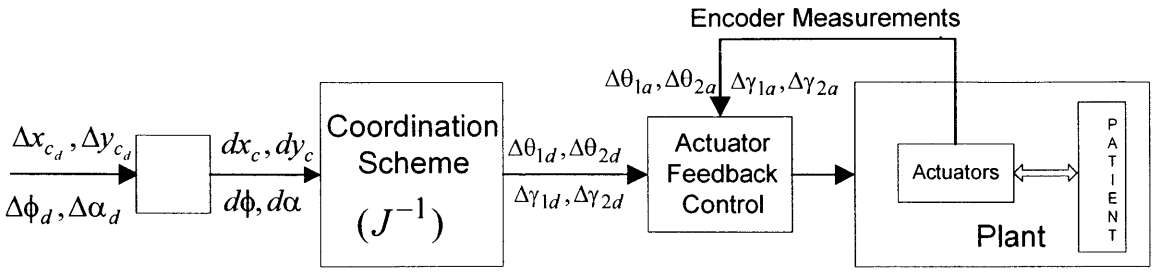


**Fig. 3.2. Feed-forward control block diagram**

It should be noted that the inverse Jacobian matrix is a function of **p** as defined in (2.47). Thus, as the patient moves, the inverse Jacobian matrix needs to be updated to correspond to the current position and orientation of the patient. However, this being an open loop scheme, the current position and orientation of the patient is not known. This difficulty is overcome by limiting the magnitudes of ($\Delta x_{cd}$, $\Delta y_{cd}$, $\Delta\phi_d$, $\Delta\alpha_d$) to ($dx_c$, $dy_c$, $d\phi$, $d\alpha$) and updating the Jacobian after each step. This assumes that the patient has indeed moved by the amounts ($dx_c$, $dy_c$, $d\phi$, $d\alpha$) following the actuator commands. However, it remains to determine the initial configuration of the patient and this can only be given approximately by an eye estimate. The joint angle commands are fed to the actuator feedback control module, which ensures that the motors follow the joint angle commands. The details of the actuator closed loop control scheme are discussed in the next section together with the closed loop control at the patient level.

The open loop scheme has several limitations because of all the factors mentioned above and we thus go in for a more reliable closed loop control scheme in the next section.

### 3.1.2 Closed Loop Control

#### *A. Sensor Feedback*

We use sensor feedback to improve the reliability of the repositioning operation. Various sensor modalities can be used for the body position and orientation measurement. An essential feature of any sensing modality is that it should not hinder the mobility of the patient in any way. Vision and optical sensors may be used if the line-of-sight requirement is satisfied. For our purpose we use a commercially available 6-axis magnetic sensor capable of measuring three position coordinates in Cartesian space and three angles of rotation about three orthogonal axes. A small sensor cube is attached to the upper chest of the patient body. This serves as a marker and its position and orientation can be sensed relative to another unit, which is mounted at a convenient location. The two units communicate through magnetic coupling and the relative position and orientation is then sent to the computer, which controls the motors. The magnetic sensor uses pulsed DC magnetic technology as opposed to AC technology and is thus less susceptible to the presence of nearby metal.

Attaching a sensor to a patient body is an acceptable technology not only for patients at hospitals and nursing homes but also for infirm and demented patients at home. Vital signs such as respiration, pulse, and saturated oxygen level are monitored with sensors worn by the patient. The magnetic sensor described above may be integrated and incorporated into those vital sign sensors. Respiration, for example, can be measured with the magnetic sensor attached to the upper chest. The optimal sensor modality should be selected by considering the total system architecture for treating a bedridden patient.

### *B. Measurements and Estimation*

Using the magnetic sensor we can directly obtain the position ($x_c$ and $y_c$) and orientation ($\phi$) information for the body. However, the angle $\alpha$, which is the angle between the two straight segments of the bed sheet, is difficult to measure directly. Yet, the knowledge of $\alpha$ is required to update the Jacobian matrix, as well as to ensure that the patient does not slip on the bed sheet. We circumvent this difficulty by using a model-based estimate of the angle $\alpha$. For this purpose, we use the magnetic sensor measurements ($x_c$, $y_c$ and $\phi$) as well as encoder measurements from motors $M_1$ and $M_2$ ($\theta_1$ and $\theta_2$ respectively) to calculate the value of $\alpha$. The straight segments of the bed sheet are tangent to the elliptical cylinder and the slopes of these tangents can be approximately calculated by assuming that they pass through the center of the rollers. This is a valid approximation because the radii of the rollers ($r_1$ and $r_2$) are much smaller than the other length scales ($D$, $l_1$, $l_2$, $a$, $b$) involved.

We first determine the centers of the rollers in the world coordinate frame and then transform to the body coordinate frame. The calculations are shown for roller 2 only and a similar result holds for roller 1. From Fig. 2.9:

$$\vec{\mathbf{OR}}_2 = \vec{\mathbf{OM}}_2 + \vec{\mathbf{M}}_2\vec{\mathbf{R}}_2 \tag{3.1}$$

In scalar form (3.1) reduces to the following equations:

$$x_2 = -D + l_2 \cos\theta_2 \tag{3.2}$$

$$y_2 = l_2 \sin\theta_2 \tag{3.3}$$

where $x_2$ and $y_2$ are the coordinates of the centers of the rollers in the world coordinate frame. Let us note that the current values of $x_2$ and $y_2$ are known from the encoder

measurement of motor $M_2$. We transform these coordinates to the body coordinate frame to get:

$$x_2^{'} = -x_c + x_2 \cos\phi + y_2 \sin\phi \tag{3.4}$$

$$y_2^{'} = -y_c + y_2 \cos\phi - x_2 \sin\phi \tag{3.5}$$

Once again, the angle $\phi$ is known from the magnetic sensor attached to the patient. Thus the coordinates are all known as functions of $\theta_2$ and $\phi$, both of which are measured quantities. In the final step, we determine the slopes of the tangents to the ellipse in the body coordinate frame as:

$$\begin{aligned} m_1^{'} &= \frac{x_1^{'}y_1^{'} \pm \sqrt{x_1^{'2}y_1^{'2} - (y_1^{'2} - b^2)(x_1^{'2} - a^2)}}{x_1^{'2} - a^2} \\ &= \tan(\beta_1 - \phi) \end{aligned} \tag{3.6}$$

$$\begin{aligned} m_2^{'} &= \frac{x_2^{'}y_2^{'} \pm \sqrt{x_2^{'2}y_2^{'2} - (y_2^{'2} - b^2)(x_2^{'2} - a^2)}}{x_2^{'2} - a^2} \\ &= \tan(\beta_2 - \phi) \end{aligned} \tag{3.7}$$

Using (2.15), (3.6) and (3.7) we may write:

$$\tan\alpha = \frac{m_1^{'} - m_2^{'}}{1 + m_1^{'}m_2^{'}} \tag{3.8}$$

Hence:

$$\alpha = \tan^{-1}\frac{m_1^{'} - m_2^{'}}{1 + m_1^{'}m_2^{'}} \tag{3.9}$$

$$0 \le \alpha \le 180$$

Thus, we have determined $\alpha$ as a function of the measured quantities. However, the result is still incomplete because of the ambiguities in the signs on (3.6) and (3.7). We resolve the ambiguities by considering the geometrical interpretation of (3.6) and (3.7). Each slope, $m_1^{'}$ and $m_2^{'}$, has two different values corresponding to the two tangents that can be drawn to the ellipse from any point. We introduce the following notation:

$$m_{ia}^{'} = \frac{x_i^{'} y_i^{'} + \sqrt{x_i^{'2} y_i^{'2} - (y_i^{'2} - b^2)(x_i^{'2} - a^2)}}{x_i^{'2} - a^2} \tag{3.10}$$

$$m_{ib}^{'} = \frac{x_i^{'} y_i^{'} - \sqrt{x_i^{'2} y_i^{'2} - (y_i^{'2} - b^2)(x_i^{'2} - a^2)}}{x_i^{'2} - a^2} \tag{3.11}$$

From the geometry of the problem, the point of intersection of the tangents $(x_A^{'}, y_A^{'})$ is in a quadrant of the body coordinate frame such that they $(x_A^{'} \text{ and } y_A^{'})$ are of the same sign, provided $\phi>0$. If $\phi<0$, they are of opposite sign. This follows from (2.21). We calculate the point of intersection as follows. Let us define:

$$c_{ia} = y_i^{'} - m_{ia}^{'} x_i^{'} \tag{3.12}$$

$$c_{ib} = y_i^{'} - m_{ib}^{'} x_i^{'} \tag{3.13}$$

The point of intersection is given by:

$$(y_A)_{jk} = \frac{m_{1j}^{'} c_{2k} - m_{2k}^{'} c_{2j}}{m_{1j}^{'} - m_{2k}^{'}} \tag{3.14}$$

$$(x_A)_{jk} = \frac{c_{2k} - c_{1j}}{m_{1j}^{'} - m_{2k}^{'}} \tag{3.15}$$

where:

$$j \neq k$$
$$j,k \in S = (a,b)$$

If $\phi$>0, we then check for the combination that satisfies:

$$(y_A)_{jk}(x_A)_{jk} > 0 \tag{3.16}$$

The corresponding slopes are chosen to evaluate (3.8).

### *C. Control Scheme*

Fig. 3.3 shows a schematic of the control scheme used to perform the task. The control scheme comprises a task planner, which supplies the desired values of the patient position and orientation. A typical example of task planning could be to alternate between the following operations:

i. Patient lies on back for 30 minutes.

ii. Patient is turned to his/her left for 30 minutes.

iii. Patient is turned to his/her right for 30 minutes.

The task planning operation is customizable to the patient. The frequency and final orientation should be determined by the caregiver according to the patient's needs. The task planner also takes into account the patient position and orientation at any instant as shown by the dotted arrows. If the patient willfully changes his/her position and is dangerously close to one side of the bed during the rest periods, the task planner can immediately detect this and reposition the patient so that they are once again in a safe position. Thus the task planner is also a safety feature of the system.

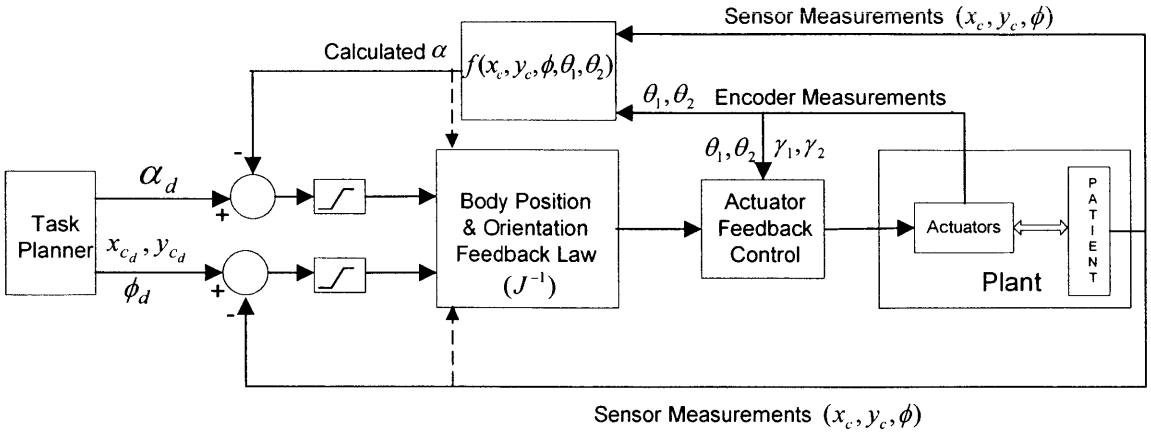


**Fig. 3.3. Schematic of closed-loop control scheme**

The inverse Jacobian matrix, as calculated in (2.72) then generates the actuator commands based on the difference between the desired and actual position/orientation. Thus, the inverse Jacobian matrix constantly updates the desired actuator angles till the difference between the desired and actual outputs go to zero. The inverse Jacobian matrix is a function of the current output variables ($x_c$, $y_c$, $\phi$ and $\alpha$) and is updated based on current sensor measurements, as shown by the dotted arrows. The value of $\alpha$ is of course estimated as mentioned in the previous section. The value of the inverse Jacobian is valid only in the neighborhood of the current position/orientation ($x_c$, $y_c$, $\phi$ and $\alpha$). The difference between the desired and actual values is passed through a saturation function before post-multiplying with the Jacobian, so as to ensure that the generated actuator angles are meaningful. The saturation function is given by:

$$\begin{aligned} sat(s) &= s \quad if \mid s \mid \leq \phi \\ sat(s) &= \phi \quad if \ s > \phi \\ sat(s) &= -\phi \quad if \ s < -\phi \end{aligned} \tag{3.17}$$

The value of $\phi$ is limited to 1mm for the linear displacements and to about .05 radians for the angular displacements. The actuator feedback control is once again the

commercially available controller for the four motors, which can drive the motors to the desired angles ($\theta_1$, $\theta_2$, $\gamma_1$ and $\gamma_2$), as generated by the inverse Jacobian matrix. The controller coordinates the speed of the motors ($\dot{\theta}_1, \dot{\theta}_2, \dot{\gamma}_1$ and $\dot{\gamma}_2$) so that the rate of change of the outputs ($\dot{x}_c, \dot{y}_c, \dot{\phi}$ and $\dot{\alpha}$) can be set to desired values. This is important, so as to ensure the comfort of the patient. This is done according to (2.71), rewritten in the form:

$$\dot{\mathbf{q}} = \mathbf{J}^{-1}\dot{\mathbf{p}} \tag{3.18}$$

## 3.2 Repositioning Operations

This control scheme was implemented by programming in Visual C++. Fig. 3.4 shows a picture of a dummy patient lying flat on the bed with the sensor attached. The general strategy used consisted of first changing $\alpha$ (without inclining the body further) so as to ensure no slip. Then the angle $\alpha$ was held constant and the body was repositioned as desired. Despite the approximate nature of the elliptical model, it turned out that the bed could successfully reposition both actual and dummy patients as desired. The actual sensor measurements of the patient's position and orientation at the end of the operation agreed well with the desired position and orientation.


**Fig. 3.4. Dummy patient with sensor attached**

Figures 3.5 and 3.6 demonstrate two snapshots of the operations involved in rolling the patient. The process of rolling involves coordination of the motions of the rollers and the arms on which the rollers are mounted. The value of $\alpha$ during this operation was restricted between 25° and 100°. The value of 100° corresponds to the start of the operation when the patient body is horizontal. As the inclination of the body to the horizontal increases, the value of $\alpha$ is gradually reduced to about 25°. For these values of

**Fig. 3.5. Initial Stage of Rolling**

$\alpha$, there was no slip between the body and the bedsheet, and a reasonable field of view was maintained for the patient. In a real-life situation the patient may wilfully change his/her orientation during such an operation. To mimic this, the patient's orientation was perturbed during the operation of rolling and it was observed that the feedback control corrected for this disturbance.

**Fig. 3.6. Final Stage of Rolling**

The operation of transferring a patient from the bed to an adjoining bed or gurney is also important. This is another job that requires substantial manual labor. We successfully demonstrated the operation of transfer of a patient to an adjoing "bed", as shown in Fig. 3.7. This was performed while keeping the position of the patient horizontal during the operation. The value of $\alpha$ was kept at around 100° since there is no chance of slip.


**Fig. 3.7. Transfer of patient to adjoining bed**

# Chapter 4
# CONCLUSION

## 4.1 Summary of Achievements

The primary objective of this thesis was to model the manipulation of a rigid body with a flexible sheet and to apply the model to accomplish the task of repositioning a bedridden patient using a flexible bed sheet. We have successfully developed a quasi-static model for the manipulation of a rigid body using the flexible sheet. The underlying concepts are elementary (geometry and statics) and it turns out from experiments that the simple models can portray the physical reality quite accurately.

The modeling is sufficiently general and can be applied to a large family of body shapes with mild assumptions (continuously differentiable bounding curve). In this work, for the sake of mathematical tractability, we have made the assumption that the body is shaped as an elliptical cylinder. The problem formulation provides an easy extension to other bounding curves, especially those, which can be expressed parametrically.

The quasi-static assumption was made keeping in mind the nature of the application at hand. The maneuvering of the patient body using the rehabilitation bed has to be performed sufficiently slowly so that the patient does not feel any discomfort.

The no-slip condition that has been developed is critical in such manipulation tasks. We provide a no-slip condition relating the body shape, the coefficient of friction, the angle

of inclination of the body to the horizontal and the angle between the straight segments of the bed sheet. The general expression is evaluated for the special case of the elliptical cylinder and the theoretical model is compared against experimental data. As seen from experiment, the theoretical model is a reasonably accurate description of the physical reality. The no-slip condition is particularly important for the bedridden patient, because slippage on the bed sheet can be particularly harmful to the patient's fragile skin. In fact, the primary purpose of the rehabilitation bed is to prevent further damage to the patient's skin and thus alleviate/prevent bedsores. The theoretical model, when used with a factor of safety can thus be deemed safe for maneuvering the patient.

The modeling was then applied to the rehabilitation bed and a control strategy for the coordination of multiple actuators to reposition the patient was provided. In particular, a methodology for the estimation of the angle between the two straight segments of the bed sheet was suggested, based on other sensor data. The knowledge of this angle is critical because it ensures that the task is carried out in the no-slip range. Experiments were conducted on a dummy patient as well as a real person and it turned out that in both cases the bed could successfully position and orient the patient. Thus we may conclude that the elliptical model, which may seem a simplistic description of the human body shape, may be accurate enough for the repositioning operations to be performed. A more complicated geometry can perhaps be considered, but the mathematical complexity involved would be far greater with minimal improvement in repositioning accuracy, which is anyway not a precision task. Furthermore, the elliptical model involves just two mean measurements of the patient body shape, whereas a more complicated geometry would make it particularly

difficult to customize it to various patient body shapes, increasing the set-up time of the device manifold.

## 4.2 Scope for Future Work

A major limitation of the present modeling is that it considers only the quasi-static case. This turns out to be adequate for repositioning operations of bedridden patients because they are performed extremely slowly. However, as a matter of academic interest or to aid other applications it may be worthwhile to look into the dynamic case. A major concern in such a scenario would be the problem of swing. It would also be rather challenging to define and develop a no-slip condition

The modeling of the problem is at a stage where the bed can successfully position test subjects in a laboratory setting. However, the rehabilitation bed is not yet ready for hospital use. We have to address certain practical issues before the bed can be used in hospitals on a regular basis.

The modeling assumes that the patient is just air-borne during the repositioning operation. This may not be acceptable to patients in a hospital setting. The modeling is rendered inadequate because the problem becomes statically indeterminate. In order to circumvent this difficulty, we would need measurements of the contact force between the patient and the bed, which would necessitate instrumentation of the surface of the bed.

The other requirement is that the bed sheets must be sufficiently sturdy to take the weight of the patient. The bed sheets currently used in hospitals are certainly not strong enough to bear the weight of the patient. If the bed sheets are even slightly damaged, they cannot be used in further operations, because the safety of the patient is jeopardized. This

may be a problem in hospital settings, because the sheets have to be washed frequently and may undergo minor wear and tear.

In conclusion, it may be said that the rehabilitation bed is indeed a versatile device, which is capable of alleviating secondary ailments of bedridden patients. It is also a valuable aid for caregivers who undergo considerable hardships while repositioning bedridden patients. However, handling human beings is extremely complex and all the issues that have been outlined must be addressed before the bed is ready for hospital use.

# REFERENCES


[1] Bartolini, G., Pisano, A., Usai, E., "Robust Control of Container Cranes: Theory and Experimental Validation," *Proceedings of the 40th IEEE Conference on Decision and Control, December 2001*

[2] Gorman, J., Jablokow, K., Cannon, D., "The Cable Array Robot: Theory and Experiment," *Proceedings of the IEEE International Conference Robotics and Automation, May 2001*

[3] Shiang, W., Cannon, D., "Optimal Force Distribution Applied to a Robotic Crane with Flexible Cables," *Proceedings of the IEEE International Conference Robotics and Automation, April 2000*

[4] Moustafa K., "Feedback Control of Overhead Cranes Swing with Variable Rope Length," *Proceedings of the American Control Conference, June 1994*

[5] Basmajian, A., Blanco, E.E., Asada, H.H., "The Marionette Bed: Automated Rolling and Reposition of Bedridden Patients," *IEEE International Conference on Robotics and Automation, 2002,* Vol. 2, 1422-1427.

[6] Shelby Hixson, RN, MSN, CCRN; Mary Lou Sole, RN, PhD, CCRN, FAAN; Tracey King, RN, BSN, CCRN "Nursing Strategies to Prevent Ventilator-Associated Pneumonia," *AACN Clinical Issues: Advance Practice in Acute and Critical Care,* Vol. 9, No 1. February 1998.

[7] http://seniors-site.com/ coping/sickdyin.html

[8] http://www.hill-rom.com

[9] http://www.kci1.com

[10] http://www.decubitus.org/cost/cost.html

[11] Garg, A., Owen, B.D., Carlson, B., "An ergonomic study of nursing assistants' job in a nursing home," *Ergonomics*, Vol. 35, no. 9, 979-995, 1992

[12] Garg, A., Owen, B. D., Beller, D., Banaag, J., "A biomechanical and ergonomic evaluation of patient transferring tasks: bed to wheelchair and wheelchair to bed," *Ergonomics*, Vol. 34, no. 3, 289-312, 1991

[13] Garrett, Singiser, and Banks, 1992. "Back injuries among nursing personnel: the relationship of personal characteristics, risk factors, and nursing practices," *AAOHN Journal*, **40** (11), 510-516.

[14] Spano, J., Asada, H.H, "Kinematic Analysis and Design of Surface Wave Distributed Actuators with Application to a Powered Bed for Bedridden Patients," *IEEE Transactions on Robotics and Automation*, Vol. 16, Issue 1, February 2000.

[15] Asada, H., Slotine, J.-J.E., *Robot Analysis and Control*

[16] Meriam, J.L., Kraige, L.G., *Dynamics*

[17] Loney, S.L., *Elements of Coordinate Geometry*

[18] Goldstein, H., *Classical Mechanics*

[19] Basmajian, A., "Design of an Assist Device for Automated Rolling and Repositioning of Bedridden Parients," *Master's Thesis,* MIT, May 2002

[20] Donald, B., Gariepy, L., Rus, D., "Distributed manipulation of multiple objects using ropes," *IEEE International Conference on Robotics and Automation, 2000. Proceedings. ICRA '00.*, Vol. 1 , 24-28 April 2000